

## Conductance and localization in a system of coupled conjugated polymer chains

S. Stafström

*Department of Physics, Linköping University, S-581 83 Linköping, Sweden*

(Received 6 June 1994; revised manuscript received 19 October 1994)

The conductance in a polymeric system of nearly macroscopic dimensions is calculated using the many-channel Büttiker-Landauer formula. A sharp decrease in the conductivity (metal-to-nonmetal transition) is observed when the length of the polymer sample exceeds some critical value. This value defines the electron localization length. For parameters that are realistic for heavily doped *trans*-polyacetylene chains, the localization length is 3–4 times the average polymer chain length.

### I. INTRODUCTION

Studies of the effects of disorder on the transport properties of inorganic semiconductors has received a tremendous amount of attention since the advent of solid-state electronics.<sup>1</sup> Parts of these studies have been focused on the conductance and the conditions for localization in one-dimensional systems.<sup>2,3</sup> It has been an issue of fundamental interest to understand these conditions; in particular, it has been shown that disorder in a one-dimensional system leads to localization, i.e., zero conductance in the limit of an infinite system,<sup>4</sup> except if the disorder is generated according to the so-called random-dimer model.<sup>5</sup> Macroscopic samples of conjugated polymers are interesting in this context since they are quasi-one-dimensional with strong intrachain interactions and weak interchain interactions. This paper is focused on the question of if these interchain interactions are large enough to allow for electron delocalization over a length scale larger than that of the individual polymer chains.

A conjugated polymer such as *trans*-polyacetylene can be doped to a conductivity that is of the same order of magnitude as those found in metals.<sup>6</sup> The observed temperature dependence of the conductivity is, however, nonmetallic in the sense that it increases with temperature.<sup>7</sup> In order to understand this behavior, we have to consider the structure of the polymer sample. On a microscopic scale the polymer chains are grouped together in weakly coupled fibrils. The general view of the electronic structure of this type of system is that the wave functions are delocalized over a single fibril only. Thus, within the fibril the conductivity is believed to be metallic but between fibrils it is thermally activated (hopping type). On the macroscopic scale, the conductivity therefore appears nonmetallic, even though other physical properties such as infrared absorption<sup>8</sup> and the response to a magnetic field<sup>9</sup> indicate a metallic state. Recently, Prigodin and Efetov showed that a metallic state can exist in a network of randomly coupled metallic fibrils if the concentration of interfibril contacts is large enough to overcome the percolation threshold.<sup>10</sup> Thus, there is a possibility for a true macroscopic metallic state in heavily doped polymeric systems. This percolation aspect of the metal-insulator transition is also discussed in some detail in Ref. 11.

The structure of the polymer fibrils provides a type of disorder that previously has not been studied in the context of electron localization. In terms of the nearest-neighbor hopping, this system is regular over relatively large length scales and with strong bonds along the chain direction. When arriving at a chain end, however, the coupling to the next chain in the forward direction is weak. Thus, the electrons are backscattered at each point of a chain interruption (chain end). In the limit of zero interchain interactions, this will naturally cause localization of the electronic states to a single chain only. However, the interchain interactions, even though they are weak at each individual site, reduce the effect of backscattering<sup>12</sup> and, as will be shown below, allow for delocalization over a length scale considerably larger than the length of the individual chains.

### II. METHODOLOGY

#### A. Calculation scheme

The many-channel Büttiker-Landauer conductance formula<sup>13</sup> is used to study the conductance as a function of the length of the system. This formula can be expressed as

$$G = \frac{e^2}{\pi\hbar} \sum_j T_j = \frac{e^2}{\pi\hbar} \text{Tr}(\tau\tau^\dagger), \quad (1)$$

where  $T_j$  is the probability for an electron incident from a perfectly conducting wire into channel  $j$  of the sample to be transmitted through the sample. The  $\tau$  matrix in Eq. (1) is a square matrix with dimension equal to the number of channels in the system. Using the transfer-matrix technique,<sup>14,15</sup> the elements of this matrix are expressed in terms of the energy of the incident electron and the parameters of the following Hamiltonian:

$$H = \sum_{i,j} \epsilon_{i,j} a_{i,j}^\dagger a_{i,j} + \sum_{i,j} t_{i,i+1} (a_{i+1,j}^\dagger a_{i,j} + a_{i,j}^\dagger a_{i+1,j}) \\ + \sum_{i,j} t_{j,j+1}^\dagger (a_{i,j+1}^\dagger a_{i,j} + a_{i,j}^\dagger a_{i,j+1}), \quad (2)$$

where  $j$  is the channel index and  $i$  the site index. Here, the channels are ordered in a square lattice such that each site has four nearest-neighbor sites on adjacent

channels to which the hopping is nonzero (see Fig. 1). We have also performed calculations on other types of crystal structures that are proposed for heavily doped *trans*-polyacetylene, but the results were shown to be essentially independent of the (small) variations in interchain interaction strength that exists between these structures.

Given the Hamiltonian, the elements of the  $\tau$  matrix are calculated in the following way. The probability amplitude for finding the electron on site  $l$  of the  $m$ th channel,  $c_{lm}$  is obtained from the solution of the Schrödinger equation  $H|c_{lm}\rangle = E|c_{lm}\rangle$ . Using Eq. (2), the equation of motion for the amplitudes is

$$\begin{pmatrix} c_{l+1} \\ c_l \end{pmatrix} = \mathbf{P}^{(l)} \begin{pmatrix} c_l \\ c_{l-1} \end{pmatrix}, \quad (3)$$

where the amplitudes in each of the  $M$  channels at a particular position  $l$  along the channels are represented by the  $M$  spinor  $\mathbf{c}_l$  with elements  $c_{l1}, c_{l2}, \dots, c_{lM}$ . The promotion matrix  $\mathbf{P}^{(l)}$  is given by

$$\mathbf{P}_{11}^{(l)} = \begin{pmatrix} E - \varepsilon_{1l} & -t_{1,2}^\perp & -t_{1,3}^\perp & \cdots & -t_{1,M}^\perp \\ -t_{2,1}^\perp & E - \varepsilon_{2l} & -t_{2,3}^\perp & & -t_{2,M}^\perp \\ \vdots & \vdots & \vdots & \ddots & \vdots \\ -t_{M,1}^\perp & & & -t_{M,M-1}^\perp & E - \varepsilon_{Ml} \end{pmatrix}. \quad (5)$$

The interchain ordering is that of a square lattice. Only nearest-neighbor interchain interactions are considered, i.e., in the actual calculation many of the matrix elements are set zero.

The promotion of the probability amplitudes from one end of the  $M$ -channel sample to the other is then obtained by setting  $l=0$  in Eq. (3) and multiplying the right-hand side of this equation by  $\mathbf{P}^{(1)}\mathbf{P}^{(2)}\dots\mathbf{P}^{(L)}$ , where  $L$  is the number of sites in each chain. By simple algebraic manipulations, the solutions at the ends of the polymeric sample can then be matched to the plane-wave solutions in the perfect conductors that are connected to the ends of this sample. These wave functions are

$$\psi(x=l, p_y, p_z)$$

$$\begin{aligned} &= \sum_{\alpha, \beta} \delta_{k_{y\alpha}, p_y} \delta_{k_{z\beta}, p_z} [A_{\alpha\beta} \exp(ik_{x\alpha\beta}l) \\ &\quad + B_{\alpha\beta} \exp(-ik_{x\alpha\beta}l)], \\ &-\infty < l < 0, \quad 1 < \alpha < M_y, \quad 1 < \beta < M_z \end{aligned} \quad (6a)$$

and

$$\psi(x=l, p_y, p_z)$$

$$\begin{aligned} &= \sum_{\alpha, \beta} \delta_{k_{y\alpha}, p_y} \delta_{k_{z\beta}, p_z} [C_{\alpha\beta} \exp(ik_{x\alpha\beta}l) \\ &\quad + D_{\alpha\beta} \exp(-ik_{x\alpha\beta}l)], \\ &L+1 < l < \infty, \quad 1 < \alpha < M_y, \quad 1 < \beta < M_z. \end{aligned} \quad (6b)$$

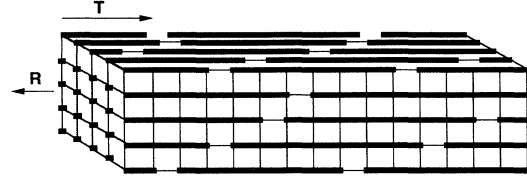


FIG. 1. Sketch of the many-channel system. Thick lines indicate the chains and thin lines sites that are weakly coupled either via interchannel couplings or end-to-end interactions.  $T$  and  $R$  denote the transmission and reflection coefficients, respectively.

$$\mathbf{P}^{(l)} = \begin{pmatrix} \mathbf{P}_{11}^{(l)} & -\mathbf{t} \\ \mathbf{1} & \mathbf{0} \end{pmatrix}, \quad (4)$$

where  $\mathbf{1}$  is the unit matrix,  $\mathbf{t}$  is an  $M \times M$  diagonal matrix with elements defined by the intrachain hopping between sites  $l$  and  $l+1$  on each of the  $M$  channels in the system [see Eq. (1)], and  $\mathbf{P}_{11}^{(l)}$  has the form

Finally, the coefficients on each side of the sample are related via the scattering matrix in the following way:

$$\begin{pmatrix} \mathbf{B} \\ \mathbf{C} \end{pmatrix} = \begin{pmatrix} \mathbf{S}_{11} & \mathbf{S}_{12} \\ \mathbf{S}_{21} & \mathbf{S}_{22} \end{pmatrix} \begin{pmatrix} \mathbf{A} \\ \mathbf{D} \end{pmatrix}, \quad (7)$$

where the coefficients in Eqs. (6a) and (6b) now are collected in the  $M$  spinors ( $M = M_y \times M_z$ )  $\mathbf{A}$ ,  $\mathbf{B}$ ,  $\mathbf{C}$ , and  $\mathbf{D}$ . The transfer matrix  $\tau$ , which relates the incoming wave on the left ( $\mathbf{A}$ ) to the outgoing wave on the right ( $\mathbf{C}$ ), is identical to the submatrix  $\mathbf{S}_{21}$  of the scattering matrix. This matrix involves the product of the promotion matrices and the exponential functions of Eq. (6). The  $\tau$  matrix can therefore be expressed in terms of the product of the promotion matrices and the wave vector of the incoming electron. Finally, the energy  $E$  of the incoming electron is introduced via its relation to the wave vector. By applying periodic boundary conditions in the plane perpendicular to the channel axis we have

$$E = 2t_0 \cos k_{x\alpha\beta} + 2t_\perp (\cos k_{y\alpha} + \cos k_{z\beta}). \quad (8)$$

Using this relation and the promotion matrices, which depend on the parameters of the Hamiltonian only, the energy-dependent conductance  $G = G(E)$  can now be calculated numerically.

## B. System

A typical width of a polymer fibril is 100–200 Å, which corresponds to a large number of chains in each

fibril. In order to simulate this in the calculations, periodic boundary conditions are applied in the plane perpendicular to the channel axis. Based on a study of the variation of conductance with the number of channels in the system (see Fig. 3 below), the number of channels is chosen to be sufficiently large to avoid any dependence on this quantity. In the results presented in Figs. 2 and 4 below, the total number of channels is 25.

Each channel contains several polymer segments separated by chain interruptions (see Fig. 1). Thus, the intrachannel hopping  $t_{i,i+1}$  involves two different types of elements, the intrachain hopping ( $t$ ) and the hopping between two adjacent chain ends ( $\delta t$ ). The intrachain hopping is usually assumed to depend linearly on the bond length between two adjacent carbon atoms.<sup>16</sup> In the heavily doped system, however, the bond-length variations along the chains are very small.<sup>17</sup> Therefore, in this work we set  $t_{i,i+1}$  equal to a constant  $t$  unless two neighboring sites in the same channel coincide with a chain interruption. By using the optimized values for the intrachain hopping, which correspond to a soliton lattice, we obtain only minor differences in the conductivity as compared to the case of a constant value of the hopping along the chain for doping levels above 12%.<sup>18</sup> Since this paper is focused on the issue of localization caused by chain interruptions and not on the detailed structure of the metallic state, we assume that the doping level is high enough so that we can neglect the differences between the real structure and the perfect metallic chain as far as the localization properties are concerned. At such doping levels, variations in the intrachain hopping caused by solitons, the potential due to the counterions, etc., all have negligible effect on the localization as compared to the effect of chain interruptions.

The chain interruptions along the channels can be caused by  $sp^3$  defects, cross linking between chains, etc. The hopping across such a chain interruption should therefore be reduced considerably compared to the intrachain hopping. It should, however, remain nonzero since some interaction between  $2p_z$  atomic orbitals is expected even though they are not participating in a chemical bond (hyperconjugation). The chain interruptions are generated at random and both rectangular and Gaussian distributions of chain interruptions are considered. The effect of the form and the width of the distribution is discussed in detail below. Calculations are performed on systems where all channels contain the same number of chain interruptions  $N$  as well as on systems with a varying number of chain interruptions per channel.

The site energies  $\epsilon_i$  and the interchain hopping  $t_{j,j+1}^\perp$  [see Eq. (2)] are assumed to be site independent. The value of  $\epsilon_i$  is therefore set to zero and the interchannel hopping is set to 0.04. (These values are realistic for *trans*-polyacetylene and correspond to an interchain hopping of 0.1 eV when the intrachain hopping is 2.5 eV.<sup>19</sup>) These site-independent values naturally represent an idealized situation as compared to the real polymeric system. However, as stated above, this work is focused on the electron-localization problem and studies have shown that weak disorder in the site energies and/or the interchain hopping are unimportant in this context as com-

pared to the effect caused by chain interruptions.<sup>12,18</sup>

The energy of the incident electron determines which state is involved in the electronic spectrum of the disordered system in the transport process. The local variations in the density of states of the disordered system will therefore cause variation in the conductance as a function of the energy of the incident electron. These variations are, however, observed to be small compared to the fluctuations caused by the different distributions of the chain interruptions. Nevertheless, the conductance values presented below are the average values obtained in an energy regime  $\Delta E = 0.1$  (in units of  $t$ ) around the Fermi energy.

### III. RESULTS

In Fig. 2 is shown the dimensionless conductance  $g = (\pi\hbar/e^2)G$  as a function of the channel length ( $L$ ). The average distance between two chain interruptions ( $\langle \ell \rangle$ ) is 200 in this case and the end-to-end hopping  $\delta t$  is 0.04. This value is identical to the interchain hopping strength (see above), i.e., the electron has the same probability to hop across a chain interruption within one channel as between chains in two neighboring channels. The set of data points for each value of  $L$  corresponds to different randomly generated distributions of chain interruptions but with the restriction that each channel contains the same number of chain interruptions. The distribution of chain interruptions is rectangular with a width equal to  $\langle \ell \rangle / 2 = 100$ . Also included in Fig. 2 are the average conductance for each value of  $L$ , and the average conductance in the case when the number of chain interruptions per channels is allowed to vary (see below).

For channel lengths less than 1000 sites, there is a very small change in the conductance even though the number of chain interruptions per channel increases from one up to three in this interval. The average conductance in this regime is in fact very close to the conductance of the perfect polymer fibril without any chain interruptions.

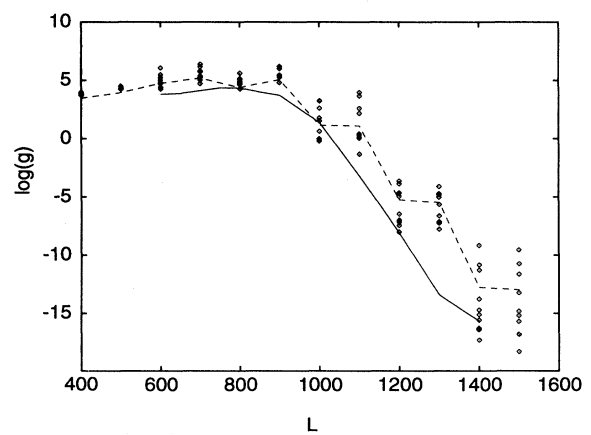


FIG. 2. Conductance ( $g$ ) as a function of the channel length ( $L$ ). The dashed line connects the average values of the conductance for each value of  $L$  and the solid line is drawn between average conductance data points for the system with a random number of chain interruptions per channel.

Clearly, the interchain interactions are important to reduce the effect of the backscattering caused by the chain interruptions.

In the case of a fixed number of chain interruptions per channel, a sharp decrease in the conductance is observed at  $L = L_C = 1000$ . The average conductance is reduced by nearly four orders of magnitude in increasing the length of the system from 900 sites per channel to 1000. This drop in the conductance corresponds to a metal-insulator transition at which the length of the channels exceeds the localization length of the electronic wave function. For the set of parameters used in this calculation, the transition occurs when the number of chain interruptions per channel is equal to four. As the length of the system is further increased we observe a staircase type of behavior of the conductance. This situation arises in the case of a fixed number of chain interruptions per channel only (cf. dashed and solid lines in Fig. 2), since in that case an increase in the number of sites in one channel from 1000 to 1100 does not increase the number of chain interruptions in the system. This shows clearly that the most relevant parameter in discussing the cause of localization in this type of system is the number of chain interruptions and not the channel length.

Naturally, in the real polymeric system, it is not realistic to have the same number of chain interruptions in all channels. Some channels might be essentially free of defects whereas others contain a large number of interruptions. The major effect of introducing a variation in the number of chain interruptions per chain comes from the channels having a large concentration of such defects. The conductance (sample average) is therefore reduced as compared to the results of the system where all channels have the same number of interruptions (see Fig. 2). Note also that the decay in the conductance above  $L = 900$  is exponential. The slope of the solid line follows closely the (average) slope of the dashed curve and could, in principle, be used to determine the localization length from the exponential relation for large  $L$ ,  $g \sim \exp(L/L_C)$ . However, this definition would result in a localization length of the order of 20 sites along the chain direction, which is somewhat inconsistent with the conductance data. The observation of a conductance that is essentially unaffected by the presence of chain interruptions up to a certain critical number of chain interruptions in the system suggests instead that the critical chain length for which the conductance starts to drop should be used to characterize the transition between diffusive and nondiffusive conductance. This chain length is here referred to simply as the critical length  $L_C$ .

As stated above, the results presented in Fig. 2 are obtained for a system of 25 channels. We have performed the same type of calculation for systems with the number of channels varying from 4 up to 100. In Fig. 3 are shown the average conductance data as a function of channel length for these systems. The results are for systems where the number of chain interruptions is allowed to vary between channels. Clearly, the conductance depends strongly on the number of channels when this number is small. The conductance shows a nearly exponential dependence of the chain length in the case of 4

channels. This dependence changes gradually into the behavior discussed above, where the conductance is essentially independent of the length of the system up to a certain critical length above which it decreases exponentially. Note that the same behavior is observed in the case of 25 and 100 channels, i.e., 25 channels is enough to represent systems with realistic fiber dimensions, at least for the concentration of chain interruptions considered here.

The unusual behavior of the conductance vs chain length shown in Fig. 2 is a result of the type of disorder considered here, as well as of the quasi-one-dimensional (quasi-1D) nature of the system. If the interchain hopping term is set equal to the intrachain hopping strength (3D case) or if the number of channels is very small (1D case, see Fig. 3), the usual type of disorder-induced exponentially localized wave functions appear. This shows that the quasi-one-dimensional nature of conjugated polymeric systems provides an example of a class of materials that differ from previously studied materials in the way the conductance responds to disorder in the form of chain interruption.

The behavior of the conductance shown in Figs. 2 and 3 above is a result of the particular type of disorder discussed here, namely, sparsely distributed for strong defect sites. As pointed out above, the essential parameter in this case is the number of such defects. In a situation where the number of defects is the same for all channels the drop in the conductance occurs when this number exceeds some critical value. In this case the conductance is essentially independent of how these defects are distributed. However, when the number of defects per channel is allowed to vary, the drop in the conductance occurs for smaller values of  $L$ , the broader the distribution of defects is. As shown in Fig. 4, the drop in the conductance curve starts already at  $L = 600$  if the defects are completely randomly distributed. (The separation between chain interruptions varies between 0 and 400 sites in this case.) This is due to the fact that channels with a larger number of defects than the average value decrease the conductance, whereas channels with the average number

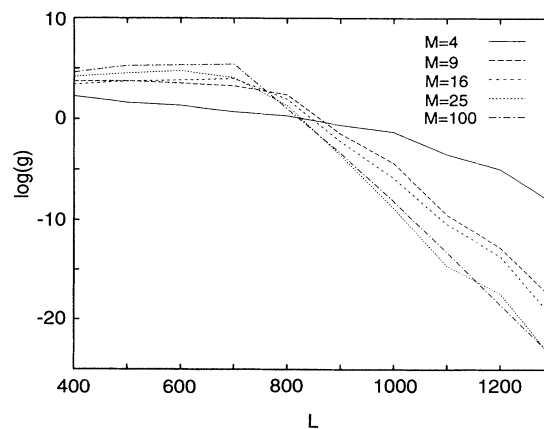


FIG. 3. Conductance vs channel length ( $L$ ) for a different number of channels  $M$  in the system.

of defects or less all have the same conductance. In Fig. 4 is also shown the calculated conductance vs  $L$  for a Gaussian distribution with a full width at half maximum (FWHM) equal to 100 which in this case corresponds to half the average separation between defects. This case results in a conductance that behaves very similarly to that of the rectangular distribution of defects with a width equal to 100 sites.

As discussed above, these interruptions could be of various types, actual chain breaks,  $sp^3$  defects, cross linking between chains, etc. A number of studies have been performed on so-called segmented polyacetylene, with a high concentration of  $sp^3$  defects. It was shown that in such systems, clustering must occur to explain the properties of this material.<sup>20</sup> In the highly conducting systems, however, the number of defects is very small, typically below 1%, and it is questionable how important clustering is in these systems. Moreover, for extremely low concentrations of  $sp^3$  defects, other types of chain interruptions are probably equally important. The fact that the Gaussian distribution of defects gives results that are very similar to those of the rectangular distribution shows that the conductance does not depend critically on the exact type of distribution and that the results presented in Figs. 2–4 are rather general.

By studying  $G$  as a function of  $\langle \ell \rangle$  and  $\delta t$ , we obtain the dependence of the localization length of the electronic wave function on these two parameters. In these studies we have chosen to use a rectangular distribution of chain interruptions. The width of the distribution is  $\langle \ell \rangle / 2$ . Furthermore, in order to facilitate the location of the critical length ( $L_C$ , see above) the number of chain interruptions is the same in all chains. One should therefore keep in mind that in a situation where the number of chain interruptions varies between chains,  $L_C$  is slightly reduced as compared to the results presented here (see Figs. 2 and 4).

For  $\langle \ell \rangle$  less than approximately 1200 sites ( $\delta t = 0.04$ )

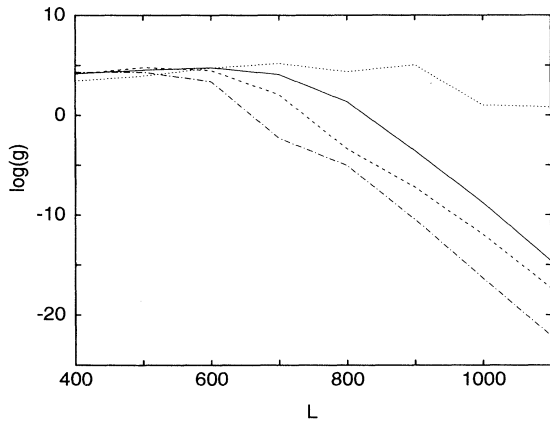


FIG. 4. Conductance vs channel length ( $L$ ) for different distributions of chain interruptions: rectangular distribution, width  $\langle l \rangle / 2$ ; constant number of chain interruptions per chain (dotted line), rectangular distribution; varying number of chain interruptions per chain, width  $\langle l \rangle / 2$  (solid line) and width  $\langle l \rangle$  (dashed-dotted line); and Gaussian distribution, FWHM =  $\langle l \rangle / 2$  (dashed line),  $\langle l \rangle = 200$  in all cases.

the transition into the metallic state is very sharp and  $L_C$  is well defined, i.e., the qualitative behavior of  $g$  is similar to that shown in Fig. 2. For larger values of  $\langle \ell \rangle$ , the transitions become more smooth and it is less obvious to define a critical length. In this case, the number of channels in the system has to be very large in order to simulate the characteristic quasi-1D behavior discussed above. This regime is practically inaccessible to numerical studies. However, in practice it is very difficult to synthesize fully conjugated segments that are much longer than those included in Fig. 5 ( $\langle \ell \rangle_{\max} = 1200$ ). The data presented here are therefore those of interest from a practical point of view.

For all values of  $\langle \ell \rangle$  included in Fig. 5 we observe a critical length of the system that is of the order of 3–4 times the average separation between chain interruptions ( $\delta t = 0.04$ ). The increase in the critical length with  $\langle \ell \rangle$  is in qualitative agreement with the large increase in conductivity observed by reducing the number of  $sp^3$  defects.<sup>5</sup> Our result also shows that coherent transport, even though it is limited by the number of chain interruptions, extends over a length scale which is larger than  $\langle \ell \rangle$ . This can explain why the mean free path of highly conducting polyacetylene, which is of the order of 600 Å,<sup>6</sup> can be considerably longer than the structural coherence length, which is around 100 Å (as obtained from x-ray diffraction studies). Note, however, that the structural coherence length is not limited by chain interruptions (e.g.,  $sp^3$  defects) only; interchain ordering and the positions of the dopant ions also play an important role in this context.

The number of chain interruptions that causes electron localization is observed to decrease for increasing values of  $\langle \ell \rangle$ . Following the solid line in Fig. 5 ( $\delta t = 0.04$ ), we notice that the first two points ( $\langle \ell \rangle = 200$  and 300, respectively) represent systems where the critical length is five times the value of  $\langle \ell \rangle$ , i.e., localization is caused by four chain interruptions ( $N_C = 4$ ). As  $\langle \ell \rangle$  increases, the value of  $N_C$  decreases as indicated by the breaks in the solid line connecting the data points in Fig. 4. Between  $\langle \ell \rangle = 400$  and 700 this value is reduced to  $N_C = 3$ , and above  $\langle \ell \rangle = 700$  two chain interruptions are enough to cause electron localization. In systems where the end-to-

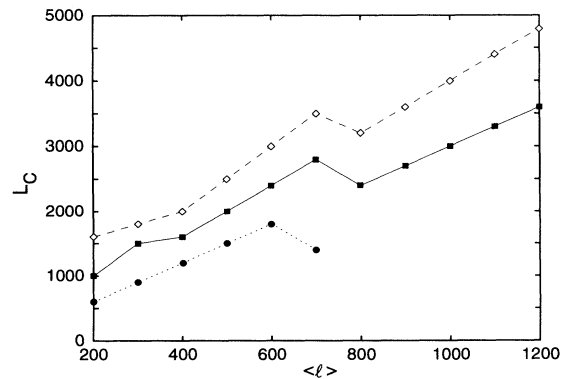


FIG. 5. Critical length ( $L_C$ ) as a function of  $\langle \ell \rangle$  for three different values of  $\delta t$ ,  $\delta t = 0.008$  (●), 0.04 (■), and 0.08 (◇).

end coupling has been doubled ( $\delta t = 0.08$ ), the value of  $N_C$  is increased by 1 except for  $\langle \ell \rangle \leq 300$  where the increase is even larger. In systems where the end-to-end coupling is very weak ( $\delta t = 0.008$ ), two chain interruptions are needed to cause localization for  $\langle \ell \rangle$  less than 600 whereas a single chain interruption causes localization for  $\langle \ell \rangle \geq 600$ . These results indicate that for infinitely long channels, a single chain interruption would cause electron localization for any value of  $\delta t$  different from the intrachain hopping strength, provided that the number of channels is finite as in this paper. In this limit the system is essentially one dimensional and this result is in agreement with the general statement that disorder of the type discussed here should lead to localization in one-dimensional systems.<sup>4</sup>

#### IV. SUMMARY AND CONCLUSIONS

In summary, the conductance in a system of coupled linear polymer chains is studied. The finite length of the polymer chains is shown to lead to a drop in the conductance for chain lengths larger than the length of the indi-

vidual chains but short as compared to typical fibril or sample dimensions. The conductance properties are different from those found in three- or one-dimensional systems. The quasi-one-dimensional nature of the system gives rise to a conductance that is constant over some region of the system and decays exponentially outside of this region.

The application of these studies are of a fundamental nature, i.e., to understand the localization properties and the conductivity in conjugated polymers. Moreover, there are a number of interesting aspects of transport in conjugated polymers that are discussed today in the context of polymer-based electronic devices, which could be studied using the approach outlined here.

#### ACKNOWLEDGMENTS

The author would like to thank the Swedish Natural Science Research Council (NFR) and the Swedish Research Council for Engineering Sciences (TFR) for the financial support of this project.

<sup>1</sup>N. Mott, *Conduction in Non-Crystalline Materials* (Clarendon, Oxford, 1987).

<sup>2</sup>R. Landauer, *Philos. Mag.* **21**, 863 (1970).

<sup>3</sup>E. N. Economou and C. M. Soukoulis, *Phys. Rev. Lett.* **46**, 618 (1981).

<sup>4</sup>D. J. Thouless, in *Ill-Condensed Matter*, edited by R. Balian, R. Maynard, and G. Toulouse (North-Holland, Amsterdam, 1980), Vol. 31.

<sup>5</sup>P. W. Phillips and H.-L. Wu, *Science* **252**, 1805 (1991).

<sup>6</sup>H. Naarmann, *Synth. Met.* **17**, 223 (1987).

<sup>7</sup>N. Basescu, Z.-X. Liu, D. Moses, A. J. Heeger, H. Naarmann, and N. Theophilou, in *Electronic Properties of Conjugated Polymers*, edited by H. Kuzmany, M. Mehring, and S. Roth (Springer-Verlag, Berlin, 1987), Vol. 76, p. 18.

<sup>8</sup>X. Q. Yang, D. B. Tanner, M. J. Rice, H. W. Gibson, A. Feldblum, and A. J. Epstein, *Solid State Commun.* **61**, 335 (1987).

<sup>9</sup>S. Ikehata, J. Kaufer, T. Woerner, A. Pron, M. A. Druy, A. Sivak, A. J. Heeger, and A. G. MacDiarmid, *Phys. Rev. Lett.*

**45**, 1123 (1980).

<sup>10</sup>V. N. Prigodin and K. B. Efetov, *Phys. Rev. Lett.* **70**, 2932 (1993).

<sup>11</sup>J. Voigt, in *Chemical Physics of Intercalation II*, edited by P. Bernier (Plenum, New York, 1993), p. 291.

<sup>12</sup>S. Kivelson and A. J. Heeger, *Synth. Met.* **22**, 371 (1988).

<sup>13</sup>M. Büttiker, Y. Imry, R. Landauer, and S. Pinhas, *Phys. Rev. B* **31**, 6207 (1985).

<sup>14</sup>A. D. Stone, J. D. Joannopoulos, and D. J. Chadi, *Phys. Rev. B* **24**, 5583 (1981).

<sup>15</sup>B. S. Andereck, *J. Phys. C* **17**, 97 (1984).

<sup>16</sup>W. P. Su, J. R. Schrieffer, and A. J. Heeger, *Phys. Rev. Lett.* **42**, 1698 (1979).

<sup>17</sup>S. Stafström, *Phys. Rev. B* **47**, 12 437 (1993).

<sup>18</sup>S. Stafström, *Synth. Met.* (to be published).

<sup>19</sup>P. M. Grant and I. P. Batra, *Solid State Commun.* **29**, 225 (1979).

<sup>20</sup>S. Jeyadev and E. M. Conwell, *Phys. Rev. B* **17**, 277 (1987).